CFD prediction of heat transfer at supercritical pressure with rough walls: parametric analyses and comparison with experimental data

S. Kassem, A. Pucciarelli ([1]), W. Ambrosini

Università di Pisa, Dipartimento di Ingegneria Civile e Industriale, Largo Lucio Lazzarino 2, 56122 Pisa,

E-mail: andrea.pucciarelli@unipi.it

ABSTRACT

In this paper, a low-Reynolds number turbulence model developed by the authors in past activities for rough walls is used for predicting heat transfer at supercritical pressure in the presence of different degrees of surface finishing. The model, able to reproduce the typical trends of friction factors from classical data reported by Nikuradse and summarised in the Moody diagram, is based on a simple-minded description of the effect of wall protrusions through the boundary layer on turbulence production.

Though prior validation of the model only on the basis of friction factor data did not assure any basis for achieving accuracy in heat transfer prediction, a sensitivity analysis is firstly presented in order to characterise the obtained predictions at variable values of the roughness parameter, in particular concerning the possible suppression of deteriorated heat transfer by roughened surfaces. These analyses are extended to different fluids, making use of a fluid-to-fluid similarity theory recently proposed by the authors in order to establish similar boundary conditions and predicted phenomena.

The results obtained by these analyses can be considered interesting, especially in view of the design of supercritical water-cooled nuclear reactors; however, an assessment against experimental data was obviously necessary. Experimental carbon dioxide data published in a very recent archival paper were thus addressed and were found useful in this regard. Considering these data allowed to extend the above analysis to provide confirmation of the promising features of the model in comparison with wall temperature values obtained with different boundary conditions. The model here described appears promising not only for its capability to predict experimentally measured effects, but also for the perspective to be used in the study of the behaviour of purposely roughened surfaces reducing the probability of occurrence of deteriorated heat transfer.

Keywords: supercritical pressure, heat transfer, rough surfaces, heat transfer deterioration

---

([1]) Corresponding Author

1. INTRODUCTION

The development of supercritical water nuclear reactors (SCWRs), a Generation IV reactor concept (see the Generation IV International Forum website), requires further advancements in knowledge of phenomena and modelling capabilities in different fields, addressing the specific needs, e.g., in terms of material resistance, neutronic design and thermal-hydraulic analyses. Reviews of existing research and available data to support model development have been presented in last decades in textbooks (see, e.g., Pioro and Duffey, 2007; Oka et al., 2010; Schulenberg and Starflinger, 2012) and in recent international reports issued in the frame of International Atomic Energy Agency (IAEA) Coordinated Research Projects (IAEA, 2014; 2019; 2020). Literature is also rich of continuously appearing papers reporting new information and modelling tools in support to the design of supercritical water reactors (Wu at al., 2022).

Among the interesting features of reactors making use of supercritical water, at a pressure generally in the range of 25 MPa, there is the fact that they are the only generation IV concept making use of the most widespread coolant adopted for nuclear reactors worldwide, being light water. This provides a good basis to believe that the wealth of experience gained in operating nuclear reactors for a great share of the present 20,000 reactor-years of operation accumulated by the world nuclear fleet can result useful in designing and operating this new reactor concept. Other relevant advantages of SCWRs are the plant simplification with respect to current PWRs, owing to the adoption of a direct cycle for energy conversion, the higher efficiency due to the higher exit fluid temperature and the absence of critical heat flux phenomena owing to operation above the critical pressure (see, e.g., Pioro and Duffey, 2007).

The latter advantage is somehow counterbalanced by the fact that predicting heat transfer and friction at supercritical pressure may result challenging when operating at temperatures close to the pseudo-critical one, where the fluid exhibits strong changes in thermodynamic and thermo-physical properties, resembling a sort of pseudo-boiling characterised by the appearance of lighter and heavier fluid regions. With respect to two-phase flow conditions, the complexity of the observed phenomena is only slightly mitigated by the absence of interfaces separating the liquid-like and the gas-like fluids, resulting in the need to upgrade models adopted for single-phase fluid conditions accounting for additional phenomena which have been observed and studied for decades. Heat transfer and friction correlations have been proposed to reflect the observed phenomena with some success, though improvements are still needed, especially to address the phenomenon of heat transfer deterioration, a decrease in the efficiency of heat transmission at the wall caused by the superposition of forced and natural convection due to buoyancy and acceleration. In vertical upward flow, these phenomena lead in some conditions to a decrease in turbulence production close to the heated surface, identified in short as "laminarization"; the occurrence of this decreased production of turbulence, combined with changes in fluid properties at the wall, shifting from liquid-like to gas-like values

of the relevant parameters, may result in larger values of wall temperatures than expected for normal heat transfer conditions at a given heat flux and coolant flow.

The experimental characterisation of deteriorated heat transfer phenomena has been proposed in milestone works by Prof. J.D. Jackson and collaborators (see, e.g., Jackson and Hall, 1979; Jackson, 2002) and continues to attract the interest of the scientific community. In previous publications, the authors of this paper have repeatedly proposed explanations of the behaviour observed in experimental data that are being collected by different researchers, aiming to gain better insight into these complex phenomena. In particular, the use of Computational Fluid Dynamics (CFD) models progressively refined in prior works (Pucciarelli and Ambrosini, 2017; 2018) allowed to identify some interesting characteristics of deteriorated heat transfer; in particular:

- a frequent type of deterioration is observed at the inlet of a heated section, when the radial velocity profile is progressively distorted by buoyancy effects; this phenomenon can be characterised by a sort of entry-length shape function, superposed to the classical one due to boundary layer build-up, that may terminate with a heat transfer recovery or may lead to higher levels of wall temperature, also in consideration of the phenomenon discussed at the next item of this list (Pucciarelli and Ambrosini, 2022);
- sharp wall temperature excursions may sometimes be observed, in similarity to what happens for critical heat flux at subcritical pressure, though they are generally less severe; in similarity with corresponding subcritical phenomena, these excursions can be explained with a reduction of the overall effective conductance, needing a shift to a higher wall temperature manifold to find a possible operating point; though supercritical pressure and subcritical pressure phenomena are obviously different, a close similarity is observed in the two cases concerning the trends of heat flux as a function of wall temperature, allowing a quantitative description of the phenomenon by a non-monotonic curve that has been meaningfully referred to have a "pseudo-Nukiyama" shape (Pucciarelli et al., 2022);
- heat transfer deterioration due to buoyancy effects can be terminated simultaneously with the transition to gas-like conditions, notwithstanding the lower value of fluid conductivity, when the difference in fluid density at the wall and in the bulk becomes sufficiently small so that buoyancy is less effective in suppressing turbulence (Buzzi et al., 2019).

These observations based on CFD analyses clarify and make more intuitive discussions that were partly already proposed in the relevant literature, visualising in a clear way their consequences in view of quantitative model development.

The more research on supercritical fluids proceeds in conjunction with SCWR design concept development, the closer the reference conditions for experiments and models become to real operating conditions. In this regard, emphasis is recently put on the effects of corrosion of fuel cladding materials, which need to be searched among those that can withstand the aggressive environment created by supercritical water at high

reactor outlet temperatures (e.g., at or above 500 °C). Specific concerns are raised also for the conditions at the pseudocritical temperature which are expected to enhance corrosion. In addition to the obvious metallurgical problems related to oxide formation, possibly causing embrittlement, corroded surfaces are expected also to have thermal-hydraulic effects that must be taken into account in modelling. On one hand, oxide formation may give rise to fouling which, in principle, should not constitute a huge problem for modelling, provided the related heat transfer resistance can be quantified in a sufficiently reliable way; on the other hand, corroded surfaces introduce perturbations in the flow close to the surface, thus affecting turbulence. The latter aspect can be predicted as somehow beneficial from the heat transfer point of view, since it is expected to promote turbulence, possibly enhancing heat transfer and delaying or ruling out heat transfer deterioration in operating conditions relevant for proposed SCWRs.

In this regard, roughness can be assumed to be a turbulence promoter, in similarity with augmented heat transfer conditions (see e.g., Mousa et al., 2021). Other phenomena related to surface irregularity and applicable to two-phase flow, as the effect of surface defects on the incipience of boiling (see e.g., Collier and Thome, 1996) or the use of "wicking or grooved" surfaces (see e.g., Rohsenow et al, 1998) have no clear counterpart at supercritical pressure, owing to the lack of surface tension in a fluid which is substantially single-phase, though with sharply variable properties.

In past activities, the authors of the present paper have developed a low-Reynolds RANS (Reynolds Averaged Navier Stokes) CFD model accounting for the effect of roughness on friction factors (Ambrosini et al., 2015). The model was based on a simple-minded explanation of the effect of roughness protrusions through the laminar sublayer, generating turbulence wakes in the buffer and turbulent regions, as bluff bodies normally do. This simple idea, after a specific calibration of relevant constants, resulted quite effective in reproducing the trends of friction factor proposed by Nikuradse (1933) and by the classical Moody diagram reported in basic textbooks on fluid mechanics. The calibration of the model was performed considering constant property fluids and only later it was tried to apply it to supercritical pressure fluid heat transfer, with not too clear results (Ambrosini et al., 2015). More recently our model was used in the frame of the EU ECC-SMART project (Joint European Canadian Chinese Development of Small Modular Reactor Technology, see the ECC-SMART Website) by colleagues from the Royal Institute of Technology in Stockholm (KTH) using their own CFD codes for supercritical pressure heat transfer applications (Li and Anglart, 2022); the relative success obtained by these applications stimulated us to implement the old model developed for the STAR-CCM+ code (Simcenter, 2018) into the currently used modified Lien k-ε (Lien et al., 1996) including the Algebraic Heat Flux Model (AHFM) (Pucciarelli and Ambrosini, 2017; 2018), to try similar applications which are the subject of this paper.

The results of the present work concerning roughness effects were initially obtained considering the experimental conditions by Kline (2017) for CO_2, which are related to smooth tubes only; so, this phase of the research was limited to identify postulated parametric trends provided by a model validated only on the basis of friction factor data for constant property fluids. After performing this initial parametric analysis, a recent paper, reporting experimental data for CO_2 with boundary conditions close to those of Kline (2017), was found and attentively considered (Chen et al. 2022). This paper shows qualitative trends of the effects of roughness which are fully coherent with the ones found in the parametric analyses. Therefore, the study was meaningfully completed with a comparison with experimental data that provided promising results, beyond the best expectations for a model developed on completely different data.

The results obtained in both phases of this study are presented in the following sections, highlighting the overall correctness of the adopted model assumptions, something that encourages to progress further in model refining for achieving better results.

2. MODEL CHARACTERISTICS AND PREVIOUS RESULTS

The adopted model benefits of two parallel experiences carried out at the University of Pisa during the last years addressing thermal-hydraulic aspects of supercritical fluids. It is based on a modified Lien et al. (1996) k-ε model adopting an AHFM for the purpose of evaluating the turbulent heat flux contributions (see e.g. Pucciarelli et al., 2017, 2018) and on the model accounting for wall roughness effects developed for Low-Re turbulence models (Ambrosini et al., 2015). Both models were separately set up in the frame of the STAR-CCM+ environment (Simcenter, 2018). The capabilities of the modified Lien et al. (1996) k-ε model adopting the AHFM were assessed in several previous works (see, e.g., Pucciarelli et al., 2017, 2018; Buzzi et al., 2019), addressing both normal and deteriorated heat transfer conditions and involving different supercritical fluids, often providing considerable improvements in predictions in front of the considered experimental data sets (see e.g. Figure 1). The roughness model parameters were initially calibrated basing on the Lien et al. (1996) k-ε model, demonstrating that the obtained modelling strategy was able to reproduce the Moody's diagram and the Nikuradse curves (see Figure 2, left) with a suitable accuracy when considering constant property fluids. The model was also applied to heat transfer to supercritical fluids, highlighting potential effects of roughness on the observed phenomena; an example of the obtained results is reported in Figure 2(right). At that time, still lacking an experimental evidence of roughness effects on heat transfer to supercritical fluids, those results could only be considered as the outcome of a numerical exercise suggesting the potential impact of wall roughness on the observed phenomena.
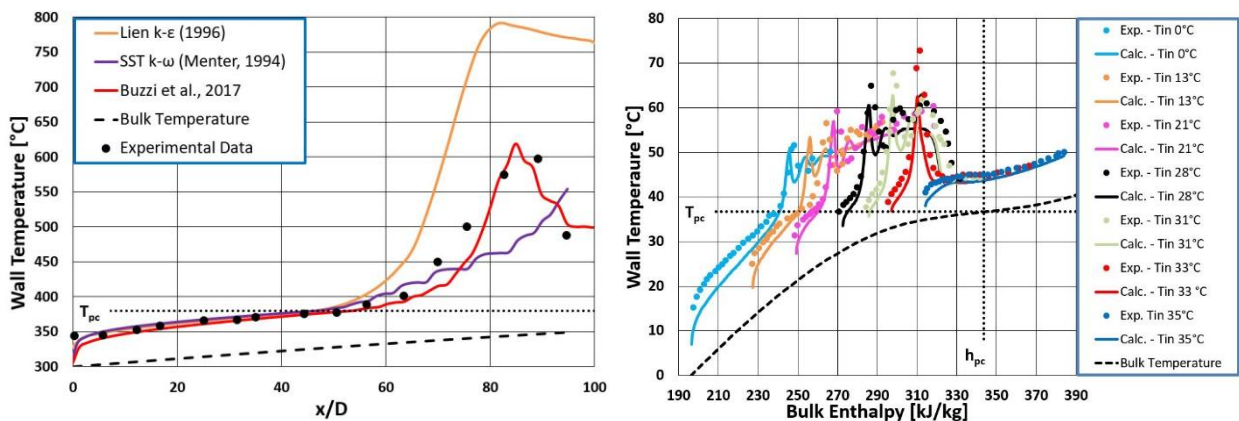

Figure 1. Examples of the predicting capabilities of the modified Lien k-ε model for two selected supercritical fluids heat transfer operating conditions: Pis'menny's data: Water at 23.5 MPa, pipe ID 6.28 mm, G = 509 kg/m2s, Tin =300 °C, q'' = 390 kW/m² (left); Klines' data: CO_2 at 8.35 MPa, pipe ID 4.6 mm, G = 300 kg/m²s, q'' = 20 kW/m² (right)
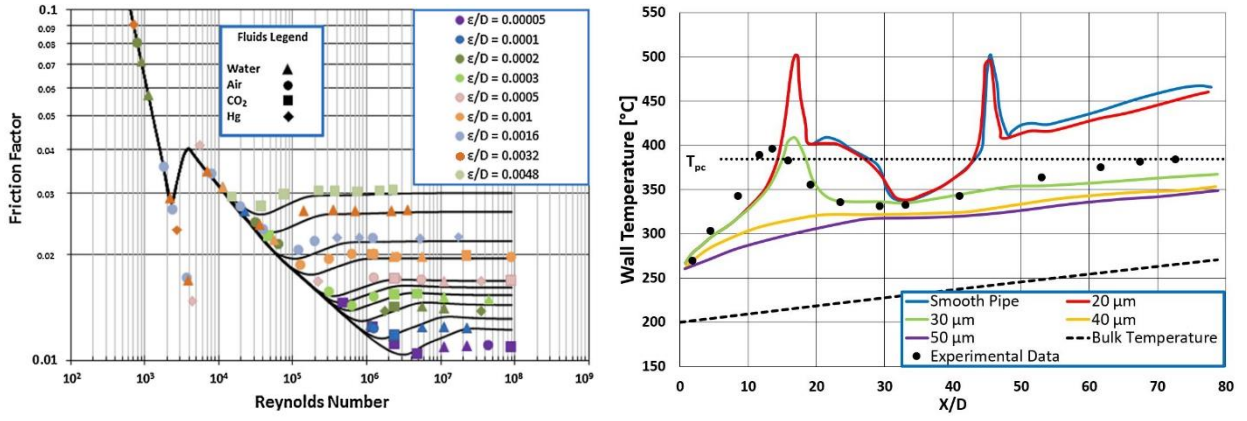
Figure 2. Nikuradse curves and the wall friction factor prediction provided by the model by Ambrosini et al. (2015) (left); and preliminary predictions of wall-roughness impact on heat transfer phenomena (right)

As a consequence, when experimental conditions investigating heat transfer to supercritical fluids for smooth and rough walls were made available in literature (Chen et al., 2022), the combination of the above mentioned models was immediately considered to assess their capabilities in such interesting operating conditions.

The main features of both components of the presently adopted model are shortly summarised hereinafter. The modified Lien et al. k-ε model for the prediction of heat transfer to supercritical fluids (Pucciarelli et al., 2018) is based on the use of the Algebraic Heat Flux Model (AHFM, Launder, 1988) for the prediction of the turbulent heat flux contributions. The adopted AHFM formulation, slightly differing from the one proposed by Launder in his work is reported below:

$$\overline{u_i' t'} = -C_t \frac{k}{\varepsilon} \left(C_{t1} \overline{u_i' u_j'} \frac{\partial T}{\partial x_j} + C_{t2} \overline{u_j' t'} \frac{\partial u_i}{\partial x_j} + C_{t3} \beta g_i \overline{t'^2} \right) \quad Eq.(1)$$

$$C_t = 1; \quad C_{t1} = 0.113; \quad C_{t2} = 0.113; \quad C_{t3} = \max \left(0, \quad e^{\frac{h_w^*}{2.5}} - 0.4 \right) \quad Eq.(2)$$

As it can be observed, the implicit relation requires the calculation of $\overline{t'^2}$, the temperature variance, which is not calculated by two-equation turbulence models. As a consequence, a dedicated transport equation for $\overline{t'^2}$ had to be included in the model using the passive scalar equation tool provided by STAR-CCM+ (Simcenter, 2018). The system is closed assuming an algebraic relation for the calculation of the dissipation of $\overline{t'^2}$, thus making the model self-standing. In addition, the C_{t3} parameter depends on h_w^*, a dimensionless wall fluid enthalpy, which proved to be a key parameter for the fluid-to-fluid scaling methodology recently proposed by the authors in publications (see e.g. Pucciarelli et al., 2020 and Kassem et al., 2021) to which the reader is referred for a more detailed description.

The turbulent heat flux contributions calculated adopting the AHFM are later adopted for the calculation of the production term of turbulence and dissipation due to buoyancy (Eq. 3) and to obtain a better estimation

of the turbulent Prandtl number distribution (Eq.4) at least in the radial direction; being the most important one for pipes and 2D channel applications:

$$G_k = g_i \overline{\rho' t'} = -\rho \beta g_i \overline{u_i' t'}; \qquad G_\varepsilon = -\frac{\varepsilon}{k} \rho \beta g_i \overline{u_i' t'} \qquad Eq.(3)$$

$$Pr_{tur} = -\frac{v_t}{\overline{u_r' t'}} \frac{\partial T}{\partial x_r} \qquad Eq.(4)$$

The model accounting for wall-roughness effects was instead developed starting from physical considerations that assume similarities between the wake generated by bluff bodies exposed to a flow and the one generated by the roughness crests (Ambrosini et al., 2015). In particular, the model was developed basing on dimensional analysis which, eventually, led to the following expressions for the turbulence production and dissipation terms induced by roughness:

$$S_{k,rough} = f_{smooth} \, C_{rough} \frac{1}{2\varepsilon_{rough}} \rho u_i^3; \qquad S_{\varepsilon,rough} = \frac{\varepsilon}{k} S_{k,rough} \qquad Eq.(5)$$

where

$$f_{smooth} = \frac{1}{2}\left[1 - tanh\left(\frac{y - \varepsilon_{rough}}{0.3\, \varepsilon_{rough}}\right)\right]; \qquad C_{rough} = 6.041 \cdot 10^{-4} \left(\frac{\varepsilon_{rough}\, u_i}{v}\right)^{0.64} \qquad Eq.(6)$$

Here, f_{smooth} represents a smoothing factor limiting the effect of roughness contributions just to the region actually occupied by the roughness crests; y is the distance from the wall and ε_{rough} is the average roughness height; C_{rough} is instead a correcting coefficient which proved to be fundamental for achieving a suitable prediction of the friction factor values at large Reynolds numbers, for different fluid and different roughness relative heights ε_{rough} /D.

The combination of the models, performed for the first time in the frame of the present work, was simply achieved by creating two global additional production contributions for the turbulent kinetic energy and its dissipation. The final production terms are thus:

$$S_{k,total} = G_k + S_{k,rough}; \qquad S_{\varepsilon,total} = G_\varepsilon + S_{\varepsilon,rough} \qquad Eq.(7)$$

The approach provided by the modified Lien et al. k-ε model for the estimation of the turbulent Prandtl number (Eq.4) was kept also in the current version of the model. As it will be remarked later, the model was applied as such to the experimental conditions recently published by Kline (2017) and by Chen et al. (2022) in their works, without any further calibration.

3. PARAMETRIC ANALYSIS FOR HEAT TRANSFER WITH DIFFERENT FLUIDS

The model described in the previous section was firstly adopted to analyse heat transfer to supercritical fluids with rough walls, without a specific reference to suitable specific experimental data which were not yet available during these first trials. The main goal of these 2D and steady-state simulations was to verify the qualitative capabilities of the model in describing the expected phenomena of heat transfer improvement owing to the effect of the source term added to the production of turbulence kinetic energy and of its dissipation.

In these first trials, the reference working conditions were drawn from the dataset collected by Kline (2017) with carbon dioxide at 8.35 MPa, flowing upwards in bare tubes of different diameters. This dataset was used in recent works by the authors in the application of a fluid-to-fluid similarity theory (Pucciarelli and Ambrosini, 2016; Pucciarelli and Ambrosini, 2020; Kassem et al., 2021; De Angelis et al., 2021) and was found very useful to allow for drawing conclusions about the relevant parametric trends, as it spans over different ranges of inlet fluid temperatures and of heat and mass fluxes.

Two-dimensional steady CFD simulations were performed adopting the low Reynolds Lien k-ε (Lien et al., 1996) turbulence model integrated with the above-mentioned Algebraic Heat Flux Model implemented in the STAR-CCM+ code and adopted as the most successful tool available to the authors for predicting heat transfer at supercritical pressure. The main assumptions about the discretisation of the pipe and the use of the low-Reynolds model are similar to those already described in Pucciarelli and Ambrosini (2018). The obtained CFD results are validated against the available experimental data for smooth tubes and, for the purpose of performing a parametric analysis, the results with different roughness heights are reported as well. In particular, Figure 3 (left) shows the wall temperature trends for one of Kline's cases at inlet temperature of 24 °C, mass flux of 300 kg/(m^{2}s), inner diameter of 4.6 mm and heat flux of 20 kW/m^2. The CFD simulation for smooth tube showed a quantitively good agreement with the experiment: though the onset of heat transfer deterioration is somehow anticipated, the overall behaviour involving deterioration, recovery and a second wall temperature peak are all predicted in good agreement with the reference experimental data for the case of smooth tube. When increasing the roughness height, the calculated wall temperature trend significantly changes and is progressively lowering; for roughness values beyond 25 μm, the second peak in wall temperature is not predicted to occur and with further increases even the first heat transfer deterioration phenomenon is not predicted anymore. These results, if confirmed by experiments, may suggest an interesting engineering solution for mitigating the problem of heat transfer deterioration, especially in view of the design of supercritical water-cooled nuclear reactors.

In order to investigate and extend the analysis to other fluids, the CFD results obtained with the similarity theory proposed by the authors (see e.g. Pucciarelli et al., 2020 and Kassem et al., 2021) by imposing similar boundary conditions were adopted and the effect of roughness was taken into consideration. Figure 3 (right)

shows the results for wall temperature of the CFD calculations made with water at 25 MPa. As it can be noted, the different heat transfer phenomena are predicted in close similarity with the ones obtained for CO_2 and show heat transfer improvement for increasing roughness height; the value of roughness at which heat transfer deterioration is disappearing is now about 36 μm for water. Similar trends are obtained for ammonia and R23, as reported in Figure 4; also in this case, the roughness strongly affects the predicted wall temperature trends and when the roughness height is 36 μm for ammonia and 23 μm for R23 the obtained results shift from the prediction of a strong heat transfer deterioration to almost normal heat transfer conditions. The similarity of the values of roughness at which deterioration disappears in the cases of CO_2 and R23, on one side, and water and ammonia, on the other, suggests a role of the similarity of the properties of the two pairs of fluids, something to be further investigated, possibly after experimental confirmation.

The effect of wall roughness was then considered in relation to the changes in the dimensionless velocity profile close to the wall, evaluated with local values of the dynamic viscosity in the classical definitions of y+ and u+ (dimensionless distance from the wall and dimensionless axial velocity). Being at supercritical pressure and having thermophysical properties that strongly change across the boundary layer also as a consequence of heat transfer deterioration, the resulting profile is deformed with respect to the classical trends. An example of velocity profile in dimensionless form for smooth wall is firstly presented for a Kline's case at T_{in} = 24 °C, while the effect of roughness is reported later. In particular, Figure 5 reports the dimensionless velocity all along the smooth pipe; as it can be noted, the velocity profile in the viscous sub-layer region is nearly the same all along the channel, though in the fully turbulent region it differs because of the intervening phenomena. At about 0.3 m, being the beginning of the heated section, the velocity in the turbulent region starts to decrease gradually, showing a plateau; by further advancing along the pipe, the flow undergoes laminarization and velocity reaches a flatter profile at about 0.5 m, which corresponds to the region where heat transfer is deteriorated. Departing from that region, the velocity is gradually increasing. In Figure 6, the velocity distribution is depicted in dimensional form as well all along the channel, clearly showing that heat transfer deterioration is attributed to the increase of flow velocity near the wall. The formation of a flattened velocity profile, which decreases the production of turbulence, confirms that laminarization of the low-density fluid layer is an important deterioration mechanism.

On the other hand, the effect of wall roughness on the characteristics of the dimensionless velocity profile is shown in Figure 7. According to what mentioned above on the flattening of the dimensionless profile due to deterioration, the curves appear distorted with respect to the usual appearance for constant property fluids: taking into account this effect, the influence of roughness can be considered.
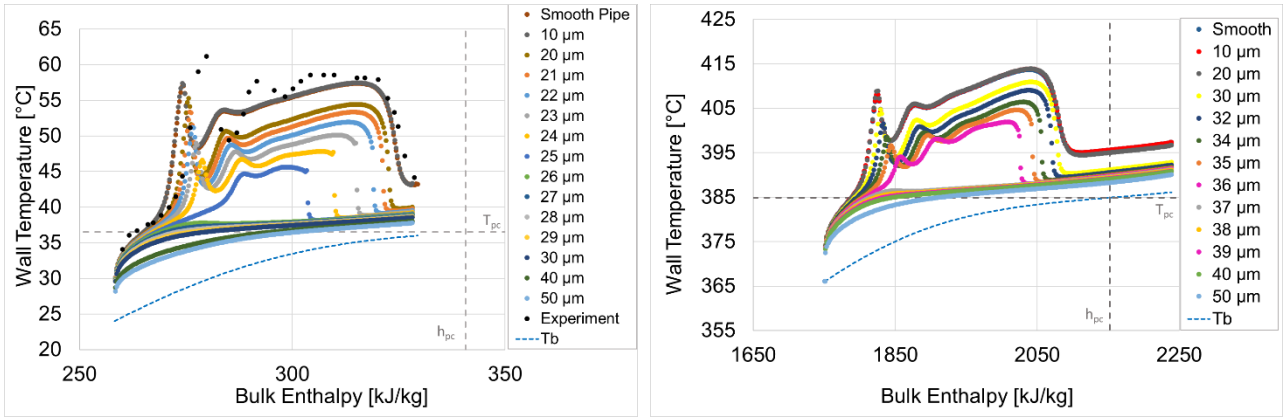
Figure 3. Wall temperature trends for Kline's CO_2 case at inlet temperature of 24 °C, mass flux of 300 kg/(m^2s), and heat flux of 20 kW/m^2 (left) and scaled case for water at 25 MPa (right) at different roughness heights
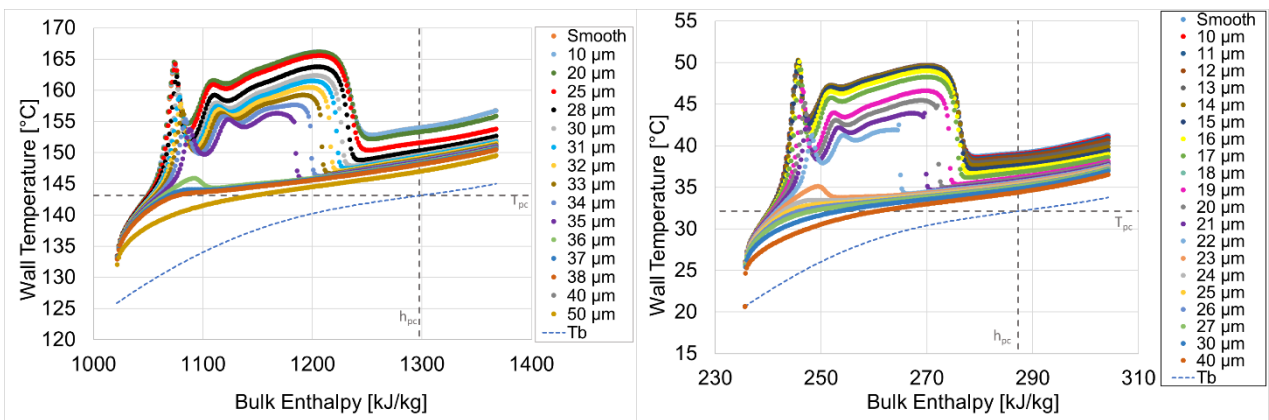

Figure 4. Wall temperature trends at different roughness heights for ammonia at 13.6 MPa(left) and R23 at 5.56 MPa(right) adopting the results from the similarity theory for Kline's CO_2 case at inlet temperature of 24 °C, mass flux of 300 kg/(m^2s), and heat flux of 20 kW/m^2
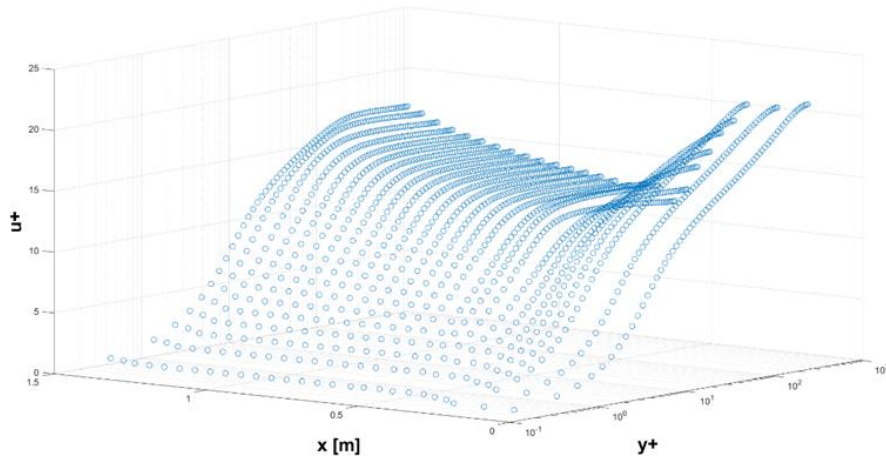
Figure 5. Dimensionless velocity trends for CO_2 at 8.35 MPa, inlet temperature 24°C, mass flux of 300 kg/(m²s), and heat flux of 20 kW/m² and with roughness 1 μm
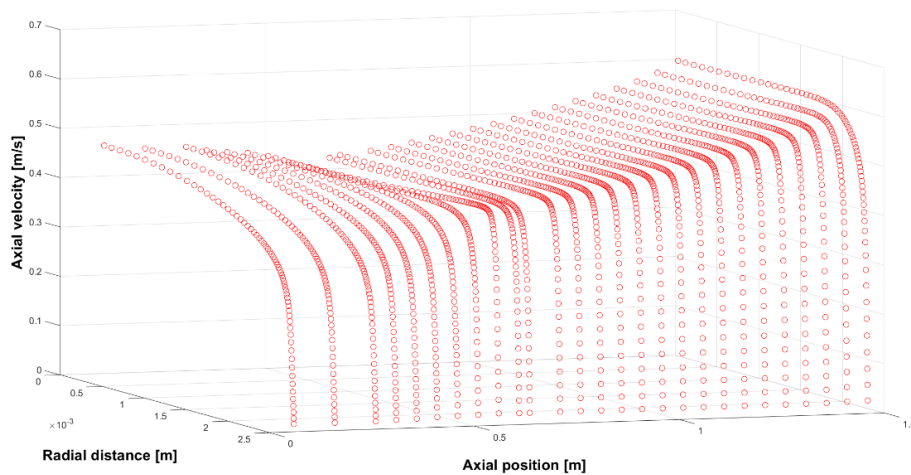

Figure 6. Axial velocity distribution across the pipe diameter for CO_2 at 8.35 MPa, inlet temperature 24°C, mass flux of 300 kg/(m²s), and heat flux of 20 kW/m² and with roughness 1 μm

At the beginning of the heated section (at 0.3 m), increasing the roughness height shows the expected dimensionless velocity distribution decrease in the buffer and fully turbulent regions. On the other hand, progressing further along the pipe in the heated region, the effect of roughness cannot be too simply inferred, as it must be combined with the possible occurrence of heat transfer deterioration phenomena. In addition, as already observed above, the presence of roughness itself may lead to the disappearance of heat transfer deterioration owing to the improved turbulent conditions. Figure 7b to Figure 7d show that for small enough roughness heights (see Figure 4 for reference) deterioration occurs, strongly distorting the velocity profiles and resulting in plateaus in the far wall region. On the other hand, increasing sufficiently the roughness height, the turbulence production may be enhanced enough to let the dimensionless velocity profile keeping the typical turbulent trend linked to to the lower degree of heat transfer deterioration, which finally disappears for sufficiently large roughness values. Once deterioration disappears, a further roughness height increase leads to the decrease of the dimensionless velocity trends in similarity with what already discussed for Figure 7a.
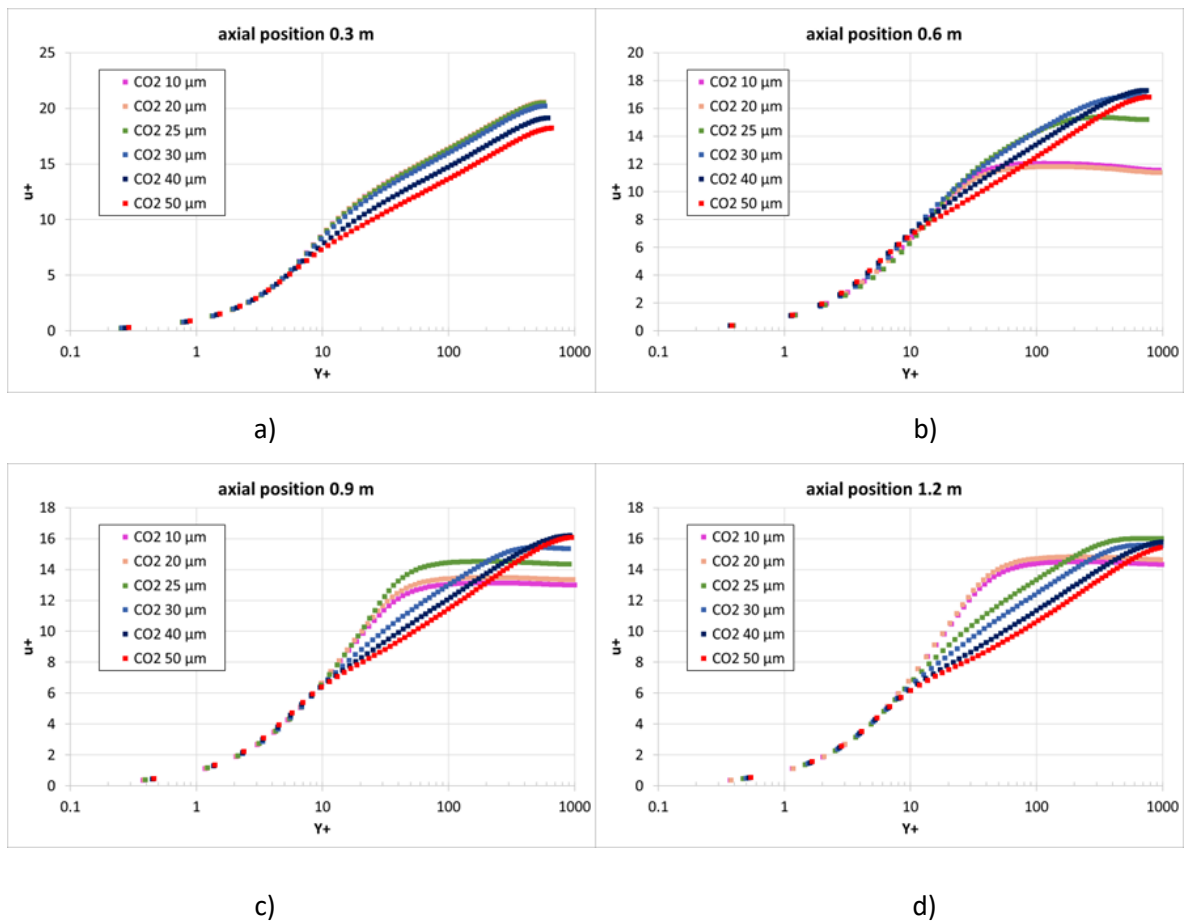
Figure 7. Dimensionless velocity trends for CO_2 at 8.35 MPa, inlet temperature 24°C, mass flux of 300 kg/(m²s), and heat flux of 20 kW/m² at different axial positions

Similarly, in Figure 8 it is shown that the dimensionless velocity profile for the corresponding case with water exhibits similar characteristics as for CO_2 while increasing the roughness height. The sequence of the described phenomena remains the same as for the reference CO_2 case but, as anticipated in the wall temperature trend analyses, the threshold roughness values are strongly affected by the different fluid properties.
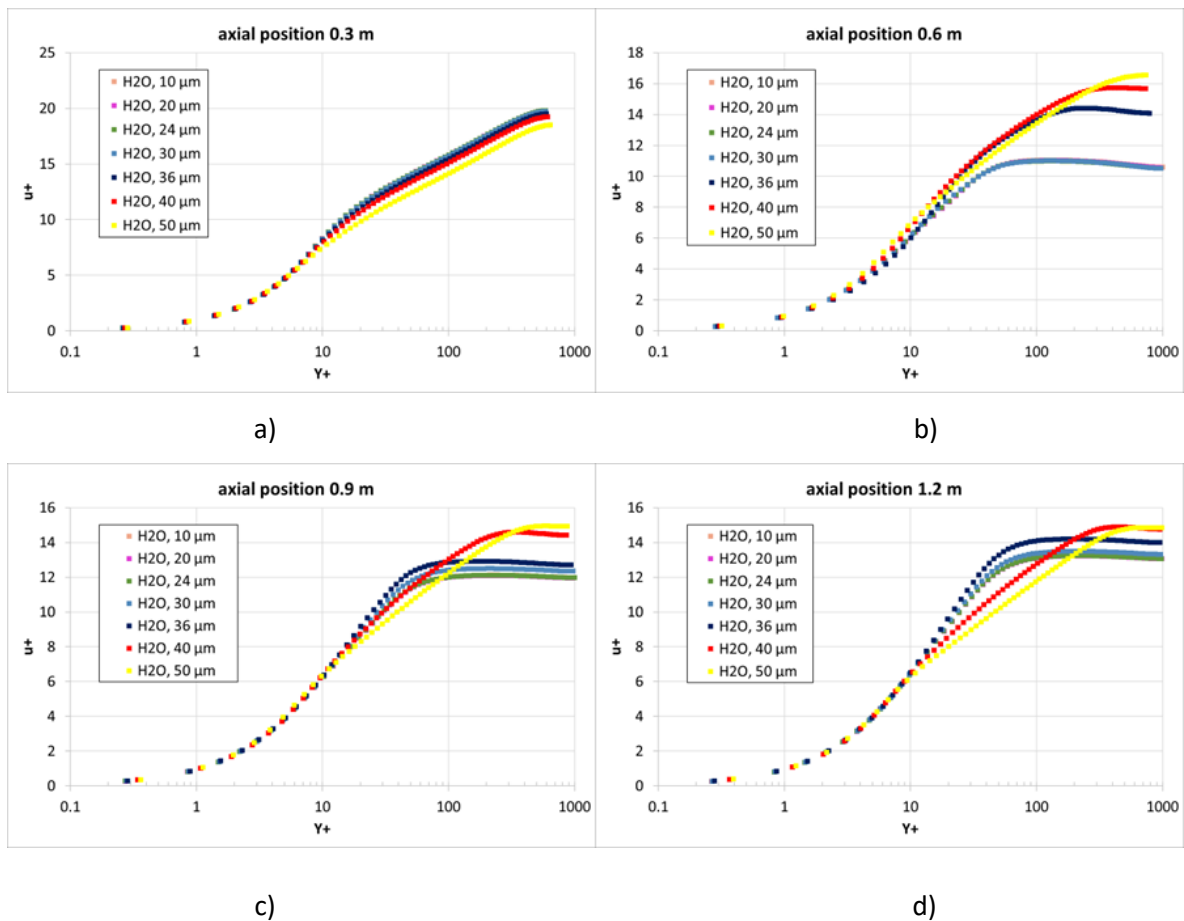
a)

b)

c)

d)

Figure 8. Dimensionless velocity trends for water at 25 MPa adopting the results from the similarity theory for Kline's CO_2 case at inlet temperature of 24 °C, mass flux of 300 kg/(m²s), and heat flux of 20 kW/m²

Globally, these data show qualitatively expected trends, whose relation to real observations must be anyway proven. This is the reason why finding a possibility of comparison in a recent paper allowed this study to reach greater significance, as described in the next section.

4. COMPARISON WITH RECENT CARBON DIOXIDE DATA ON WALL ROUGHNESS EFFECT

Chen et al. (2022) reported experimental data on the effect of roughness on heat transfer to supercritical carbon dioxide flowing upwards in vertical tubes with inner diameter of about 4.57 mm. The addressed range of the Reynolds number is $16207 \leq Re \leq 91735$ and the experiments involved various roughness heights, from 1.5 μm to 40 μm. In their study, Chen et al. (2022) clearly showed that wall roughness helps alleviating heat transfer deterioration offering a good opportunity to quantitatively assess the developed CFD model and its discussed qualitative predictions against experimental data. In general terms, in fact, the data reported by Chen et al. (2022) are strikingly similar to the ones obtained in our parametric analysis.

Five different inlet boundary conditions are considered in the present analyses with the CFD model, changing the values of the mass fluxes while imposing the same value of the heat flux. Table 1 summaries the boundary conditions for the test cases considered here, while Figure 9 to Figure 11 show the comparison of the calculated and predicted temperature profiles at different roughness and mass flux values.

As it can be noted, in general qualitative terms the model correctly reproduces the phenomenon of the increase in heat transfer efficiency with increasing roughness, up to the suppression of deterioration, as well as the anticipation of the final recovery of heat transfer due to turbulence restart. In particular, in Figure 9 (both left and right) it can be noted that for smooth surfaces the latter phenomenon occurs when buoyancy effects decrease owing to the closer values of bulk and wall fluid density, indicated in the figure by the fact that the bulk temperature approaches the pseudocritical value, T_{pc}, while the wall temperature is above it. On the contrary, for rough surfaces both experiments and analyses show an earlier turbulence restart at values of bulk temperature still far enough from T_{pc}, in strict similarity with what predicted by the model also for Kline's (2017) data (see the previous section). This is a clear effect of the additional turbulence produced by roughness: both experiments and predictions agree in depicting it, although at different values of roughness. In particular, it must be mentioned that no changes occur in the predicted trends for roughness heights smaller than of 10 μm while in the experimental data differences can be observed with respect to the smooth tube case. For both the effects of turbulence restart and suppression of heat transfer deterioration, while the values of roughness at which they occur are in the same range in both cases (a few tens of microns), the exact values for their occurrence are different in the model and the experiment, due to the limited accuracy achieved so far.

Similar behaviour with somehow larger discrepancies between experiments and predictions is shown in Figure 10 . At these higher flow rates, the model is known to be less accurate even for smooth tubes (Buzzi et al., 2019), thus justifying the limited agreement here observed. In particular, in Figure 10 (right) the suppression of deterioration due to increasing roughness occurs for higher values of ε_{rough} than in the experiments and a double oscillation in wall temperature is mostly predicted, while the experiments show a

single oscillation at low wall roughness. Figure 11 also shows discrepancies at low roughness values, but more correct trends are predicted at larger roughness parameter values. The great sensitivity of the phenomena to details in the boundary conditions, noted in many such applications, certainly also plays a role in the quality of the comparison of predictions to experimental values. Nevertheless, the capability of the adopted model in reproducing the transitions from deteriorated to normal heat transfer conditions is again confirmed.

Table 1. Boundary conditions for the selected analyses

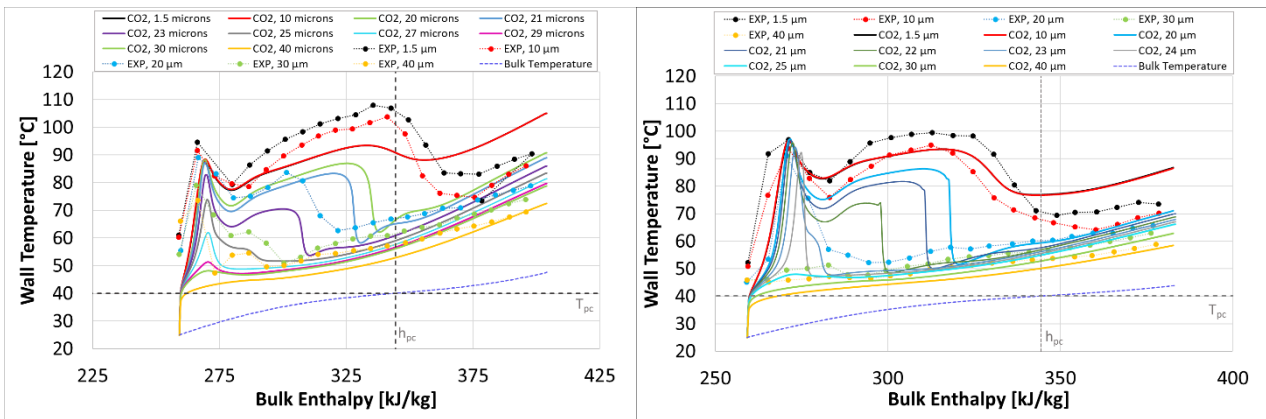| Pressure [MPa]	Inlet Temperature [°C]	Heat flux [kW/m^2]	Mass flux [kg/m^{2}s]	Roughness height [μm]
9.0	25	50	300,350,400, 450,500	1.5,10,20, 30,40

Figure 9. Wall temperature profiles with different roughness for CO$_2$ at 9 MPa, inlet temperature 25°C, heat flux of 50 kW/m^{2}and mass fluxes of 300 kg/m^{2}s (left) and 350 kg/m^{2}s (right)

Figure 10. Wall temperature profiles with different roughness for CO$_2$ at 9 MPa, inlet temperature 25°C, heat flux of 50 kW/m^{2}and mass fluxes of 400 kg/m^{2}s (left) and 450 kg/m^{2}s (right)
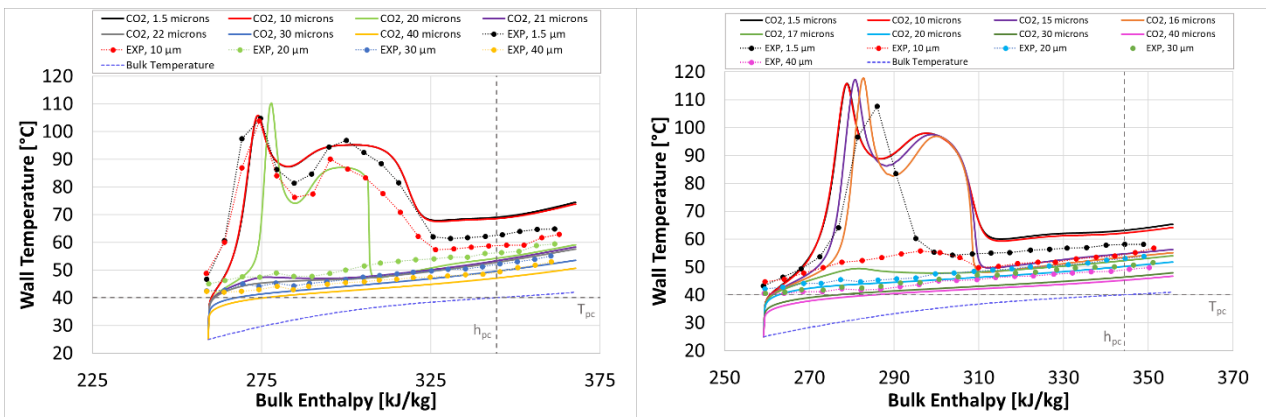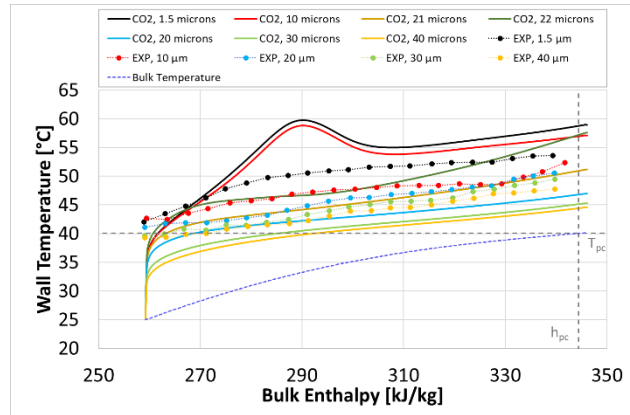
Figure 11. Wall temperature profiles with different roughness for CO_2 at 9 MPa, inlet temperature 25°C, heat flux of 50 kW/m²and mass flux of   500 kg/m²s

In summary, considering the obtained results, it can be noted that the model predicts in a reasonable way the decrease of the wall temperature due to increasing roughness, though discrepancies do appear in detailed trends. In particular, it can be observed that:

- a too low sensitivity of the model to roughness is noted at small values of the roughness parameter, between 1.5 and 10 μm, where it predicts almost the same trends, while the experiments show a decreasing wall temperature with increasing roughness;

- nevertheless, the anticipation of heat transfer restoration after deterioration because of increasing roughness occurs at similar values of the roughness parameter, though the experiments allow only a partial comparison with predictions for the limited values of roughness heights adopted in the collection of data;

- the suppression of deterioration at large enough roughness values is another common feature of the predictions and the experimental data, occurring for comparable values of roughness heights.

In summary, the present comparison with experiments looks promising, especially considering that the modelled roughness effects were initially validated only on friction factor data for constant property fluids. Though the model must be better calibrated on experimental data, it seems that it possesses the right physical features to be successful in predicting the addressed effects.

5. CONCLUSIONS AND FUTURE PERSPECTIVES

The results presented in the previous sections show the capabilities of a low-Reynolds number model that, developed on the basis only of friction factor data, appears to have the right features to also correctly predict the effect of superficial roughness on heat transfer at supercritical pressure conditions. In particular, the model shows an increase of heat transfer effectiveness owing to the increased turbulence due to roughness, especially in deteriorated heat transfer conditions, in qualitative and, at some extent, quantitative similarity to what experimentally observed, including the anticipation of the final heat transfer restoration at the transition to gas-like fluid in bulk.

Some insensitivity of the model to low values of roughness (e.g., from 1.5 to 10 μm) contrasts with the trends shown by the experimental data, suggesting areas of improvement. It must be also considered that experiments provide data only for selected values of roughness (i.e., in steps of 10 μm) while the model can be used with continuous values of the roughness height; in this regard, the known sensitivity of supercritical pressure heat transfer phenomena to details in the boundary conditions as, e.g., in the sudden suppression of deteriorated heat transfer, introduce uncertainties in the effectiveness of the comparison that must be prudently considered in having a feedback on the model. Moreover, it must be also considered that it is not possible at the present time to achieve a better characterisation of the statistical distribution of roughness surface irregularities, which could guide in defining the smoothing factor introduced in the model.

In addition to what it was done in this first application, indeed the model can be finely calibrated on the newly released experimental data to make it more coherent with them. This work is being planned as the next step in this research, hopefully making use of a wider basis of experiments that could be released in the next future also in the frame of the EU ECC-SMART project.

ACKNOWLEDGEMENTS

NOMENCLATURE

Latin Letters

C_{rough}	Correcting coefficient adopted in the roughness model
C_t, C_{t1}, C_{t2}, C_{t3}	Parameters of the AHFM model
D	Pipe Inner Diameter [m]
f_{smooth}	Smoothing function adopted in the roughness model
g	Gravity acceleration [m/s^2]
G_k, G_ε	Production terms of turbulence [kg/ms^3] and dissipation [kg/ms^4] due to buoyancy
h_w^*	Dimensionless wall enthalpy
k	Turbulent kinetic energy [m^2/s^2]
Pr_{tur}	Turbulent Prandtl Number
$S_{k, rough}$, $S_{\varepsilon, rough}$	Production terms of turbulence [kg/ms^3] and dissipation [kg/ms^4] due to roughness
u	Velocity [m/s]
T	Temperature [K]
t'	Temperature fluctuation [K]
$\overline{t'^2}$	Temperature Variance [K^2]
y	Distance from the wall [m]

Greek Letters

β	Isobaric fluid expansion coefficient at the pseudocritical threshold [1/K]
ε	Turbulent Dissipation Rate [m^2/s^3]
ε_{rough}	Average roughness crests height [m]
v	Molecular kinematic viscosity [m^2/s]
v_t	Turbulent Viscosity [m^2/s]
ρ	Density [kg/m^3]

Superscripts

+	Dimensionless
b	Bulk

Superscripts

i	i[th] direction
r	Radial direction

REFERENCES

Ambrosini, W., A. Pucciarelli, and I. Borroni., 2015. A methodology for including wall roughness effects in k-ε low-Reynolds turbulence models-Part I and Part II: Part I. Basis of the methodology. Nuclear Engineering and Design 286 (2015): 175-194.

Buzzi, F., Pucciarelli, A., Ambrosini, W., 2019. On the mechanism of final heat transfer restoration at the transition to gas-like fluid at supercritical pressure: A description by CFD analyses, Nuclear Engineering and Design 355 (2019) 110345.

De Angelis, A., Pucciarelli, A., Kassem, S., Ambrosini, W., 2021, Advances in the development of a fluid-to-fluid similarity theory for fluids at supercritical pressure: results from sensitivity analyses, Proceedings of the 2021 28th International Conference on Nuclear Engineering, ICONE28, August 4–6, 2021, Virtual, Online, ICONE28-64713.

Chen, J., Yang, S. G., Zhao, R., & Cheng, W. L., 2022. Experimental study on the effect of wall roughness on heat transfer characteristics of supercritical carbon dioxide in vertical tubes. International Journal of Heat and Mass Transfer, 196, 123258.

Collier, J.G. and Thome, J.R., 1996, Convective boiling and condensation, Third edition, Oxford University Press, Reprinted in 1999.

ECC-SMART Project Website, https://ecc-smart.eu/

Generation IV International Forum website, https://www.gen-4.org/gif/

Haipeng Li, Henrik Anglart, 2022, Presentation of KTH for Task 3.3.5 at the WP3 Meeting of ECC-SMART, May 31, 2022

INTERNATIONAL ATOMIC ENERGY AGENCY, 2014. Heat Transfer Behaviour and Thermohydraulics Code Testing for Supercritical Water Cooled Reactors (SCWRs), IAEA-TECDOC-1746, IAEA, Vienna (2014).

INTERNATIONAL ATOMIC ENERGY AGENCY, 2019. Status of Research and Technology Development for Supercritical Water Cooled Reactors, IAEA-TECDOC-1869, IAEA, Vienna (2019).

INTERNATIONAL ATOMIC ENERGY AGENCY, 2020. Understanding and Prediction of Thermohydraulic Phenomena Relevant to Supercritical Water Cooled Reactors (SCWRs), IAEA-TECDOC-1900, IAEA, Vienna (2020).

Jackson, J.D., Hall, W.B., 1979. Forced convection heat transfer to fluids at supercritical pressure, Inst. Mech. Eng. Conf. Publ. 2 (1979) 563–611.

Jackson, J.D., 2002, Consideration of the Heat Transfer Properties of Supercritical Pressure Water in Connection with the Cooling of Advanced Nuclear Reactors, Proceedings of the 13th Pacific Basin Nuclear Conference (PBNC 2002), Shenzhen City, China, 21–25 October 2002

Kassem, S., Pucciarelli, A., Ambrosini, W. 2021, Insight into a fluid-to-fluid similarity theory for heat transfer at supercritical pressure: results and perspectives. Int. J. Heat Mass Transf. 2021, 168, 120813.

Kline, N., 2017. An experimental study on heat transfer deterioration at supercritical pressures. MSc thesis. Ottawa-Carleton Institute for Mechanical and Aerospace Engineering, University of Ottawa, Ottawa Canada.

Launder,1988. On the computation of convective heat transfer in turbulent complex flows. J. Heat Transfer, 110 (1988), pp. 1112-1128.

Lien, F.S., Chen, W.L., Leschziner, M.A., 1996. Low-Reynolds number eddy viscosity modelling based on non-linear stress-strain/vorticity relations. In: Proceedings of the 3rd Symposium on Engineering Turbulence Modelling and Measurements, 27–29 May, Crete, Greece.

Mousa, M. H., Miljkovic, N., Nawaz, K., 2021, Review of Heat Transfer Enhancement Techniques for Single Phase Flows, Renewable and Sustainable Energy Reviews, Volume 137, March 2021, 110566

Nikuradse, J. 1933, Stromungsgesetze in rauhen Rohren. VDI Forschungsheft, no. 361. 1950, English Translation, NACA-TM 1292

Oka, Y., Koshizuka, S., Ishiwatari, Y., Yamaji, A., 2010. Super Light Water Reactors and Super Fast Reactors: Supercritical-Pressure Light Water Cooled Reactors. Springer.

Pioro, I.L., Duffey, R.B., 2007. Heat Transfer and Hydraulic Resistance at Supercritical Pressure in Power Engineering Applications. ASME Press, New York.

Pucciarelli, A., Ambrosini, W., 2016. Fluid-to-fluid scaling of heat transfer phenomena with supercritical pressure fluids: Results from RANS analyses, Annals of Nuclear Energy 92 (2016) 21–35.

Pucciarelli, A., Ambrosini, W., 2017, Improvements in the prediction of heat transfer to supercritical pressure fluids by the use of algebraic heat flux models, Annals of Nuclear Energy, Volume 99, January 2017, Pages 58-67.

Pucciarelli, A., Ambrosini, W., 2018. Use of AHFM for simulating heat transfer to supercritical fluids: application to carbon dioxide data. International Journal of Heat and Mass Transfer, Vol. 127, Part B (2018), 1138-1146.

Pucciarelli, A., Ambrosini, W., 2020, A successful general fluid-to-fluid similarity theory for heat transfer at supercritical pressure, International Journal of Heat and Mass Transfer, Volume 159, October 2020, 120152.

Pucciarelli, A., Ambrosini, W., 2022, A shape function approach for predicting deteriorated heat transfer to supercritical pressure fluids on account of a thermal entry length phenomenon, Nuclear Engineering and Design, 2022, 397, 111923

Pucciarelli, A., Kassem, S., Ambrosini, W., 2022, Characterisation of observed heat transfer deterioration modes at supercritical pressure with the aid of a CFD model, Annals of Nuclear Energy, 2022, 178, 109376

Rohsenow, W. M., Hartnett, J. R., and Cho, Y. I., 1998, Handbook of Heat Transfer, McGraw Hill, Third edition.

Schulenberg, T., Starflinger, J., 2012. High Performance Light Water Reactor: Design and Analyses. KIT Scientific Publishing.

Simcenter STAR-CCM+®, Documentation, Version 13.06. ©2018 Siemens PLM Software.

Wu, P., Ren, Y., Feng, M., Shan, J., Huang, Y., Yang, W., 2022, A review of existing SuperCritical Water reactor concepts, safety analysis codes and safety characteristics, Progress in Nuclear Energy 153 (2022) 104409